

Published in final edited form as:

Gut. 2014 May ; 63(5): 711–719. doi:10.1136/gutjnl-2012-303731.

Nrf2 deficiency impairs the barrier function of mouse esophageal epithelium

Hao Chen¹, Yuhui Hu¹, Yu Fang^{1,2}, Zorka Djukic³, Masayuki Yamamoto⁴, Nicholas J. Shaheen³, Roy C. Orlando³, and Xiaoxin Chen^{1,3,5}

¹Cancer Research Program, JLC-BBRI, North Carolina Central University, Durham, NC 27707, USA.

²Department of Cardiovascular and Thoracic Surgery, The Second Xiangya Hospital, Central South University, Changsha, 410011, China

³Division of Gastroenterology and Hepatology, Center for Esophageal Diseases and Swallowing, Department of Medicine, University of North Carolina, Chapel Hill, NC 27599, USA.

⁴Department of Medical Biochemistry, Tohoku University Graduate School of Medicine, Sendai, Japan 980-8575

Abstract

Objective—As a major cellular defense mechanism, the Nrf2/Keap1 pathway regulates expression of genes involved in detoxification and stress response. Our previous study revealed activation of the Nrf2/Keap1 pathway at the maturation phase during mouse esophageal development, suggesting a potential function in epithelial defense. Here we hypothesize that Nrf2 is involved in the barrier function of esophageal epithelium, and plays a protective role against gastroesophageal reflux disease (GERD).

Design—Human esophageal biopsy samples, mouse surgical models and Nrf2^{-/-} mice were used to assess the role of the Nrf2/Keap1 pathway in esophageal mucosal barrier function. Trans-epithelial electrical resistance (TEER) was measured with mini-Ussing chambers. Hematoxylin and eosin (HE) staining and transmission electron microscopy were used to examine cell morphology, while gene microarray, immunohistochemistry, Western blotting and ChIP analysis were used to assess the expression of pathway genes.

Results—Nrf2 was expressed in normal esophageal epithelium and activated in GERD of both humans and mice. Nrf2 deficiency and gastroesophageal reflux in mice, either alone or in combination, reduced TEER and increased intercellular space diameter in esophageal epithelium. Nrf2 target genes and gene sets associated with oxidoreductase activity, mitochondrial biogenesis and energy production were down-regulated in the esophageal epithelium of Nrf2^{-/-} mice. Consistent with the antioxidative function of Nrf2, a DNA oxidative damage marker (8OHdG) dramatically increased in esophageal epithelial cells of Nrf2^{-/-} mice compared with those of wild-type mice. Interestingly, ATP biogenesis, Cox IV (a mitochondrial protein) and Claudin-4 (Cldn4) expression were down-regulated in the esophageal epithelium of Nrf2^{-/-} mice, suggesting that energy-dependent tight junction integrity was subject to Nrf2 regulation. ChIP analysis confirmed the binding of Nrf2 to Cldn4 promoter.

⁵Corresponding authors: Cancer Research Program, Julius L. Chambers Biomedical Biotechnology Research Institute, North Carolina Central University, 700 George Street, Durham, NC 27707, USA. Tel: 919-530-6425; Fax: 919-530-7780; lchen@nccu.edu.

COMPETING INTERESTS Support provided by Takeda Pharmaceuticals U.S.A., Inc. The publication does not present a risk to Takeda's intellectual property rights.

Conclusion—Nrf2 deficiency impairs esophageal barrier function through disrupting energy-dependent tight junction. Elucidating the role of this pathway in GERD has potential implications for the pathogenesis and therapy of the disease.

Keywords

Nrf2; esophagus; TEER; GERD

INTRODUCTION

The barrier function of the stratified squamous epithelium of the esophagus is very important to protect the organism from the environment. The intrinsic resistance of esophageal epithelium is composed of three compartments:¹ (1) Pre-epithelial defense including the mucus layer (minimal to non-existent), unstirred water layer, and surface bicarbonate ion concentration; (2) Epithelial defense including cell membranes, intercellular junctional complex (tight junctions, glycoprotein matrix and buffers), intracellular buffers, and membrane ion transporters; (3) Post-epithelial defense including blood flow and acid-base balance. Any defects of one or more of these defense mechanisms contribute to gastroesophageal reflux disease (GERD), which is manifested as damage to the esophageal epithelium from exposure to the gastrointestinal refluxate.² Therefore, studies on the molecular aspects of these defense mechanisms may help us develop strategies to improve the esophageal barrier against gastroesophageal reflux.

As a major cellular defense pathway, the Nrf2 (Nfe2l2, nuclear factor erythroid-derived 2-like 2) pathway is known to regulate expression of enzymes involved in detoxification and anti-oxidative stress response.³ Nrf2 forms heterodimers with small Maf proteins and binds to the antioxidant response elements (ARE) of target genes when cells are exposed to oxidative stress or xenobiotics. Keap1 (Kelch-like ECH-associated protein 1) regulates the function of Nrf2 by retaining Nrf2 in the cytoplasm under normal physiological conditions, and by allowing nuclear translocation of Nrf2 under stress conditions.⁴ Interestingly, constitutive activation of Nrf2 in Keap1^{-/-} mice led to hyperkeratosis in the esophagus and forestomach.⁵ Our gene expression array data revealed that Nrf2/Keap1 pathway was activated at the maturation phase during mouse esophageal epithelial development.⁶ At this phase, the keratinized stratified squamous epithelium continues to thicken and finally forms the esophageal epithelium in adults. Since the keratinized layer is the major protective layer against physical stress and chemical injuries,⁷ and terminally differentiated keratinocytes express proteins which can provide protection by quenching reactive oxygen species,⁸ we hypothesized that Nrf2 may be involved in esophageal epithelial barrier function, and may therefore play a protective role during gastroesophageal reflux.

In this study, we observed Nrf2 expression in normal esophageal epithelium and its activation in GERD of both humans and mice. Nrf2^{-/-} mice were then compared with wild-type mice for esophageal barrier function, morphology, and gene expression in the presence of gastric, duodenal or mixed reflux. Our study demonstrated that Nrf2 deficiency impaired esophageal barrier function through disrupting energy-dependent tight junction.

METHODS

Human tissue samples

Ten pairs of biopsy tissue samples of normal esophagus and non-erosive GERD diagnosed by a gastroenterologist were obtained during routine upper endoscopy from the outpatient endoscopy suites of the University of North Carolina Hospitals. Patients with non-erosive reflux disease all had at least one previous endoscopy while off all antisecretory therapy for

at least 4 weeks which demonstrated no mucosal breaks. At the time of the study endoscopy, all GERD patients were on proton pump inhibitors for at least 2 month duration, but continuing to experience some symptoms of GERD (heartburn and/or regurgitation). All patients and controls were Caucasian males. The mean age of GERD patients was 63 yrs (SD 3.6) and of controls 57 yrs (SD 4.4). Biopsy tissue samples were harvested during from the 5 cm proximal to the GE junction on endoscopic examination. Use of human samples was approved by the Institutional Review Board. All human samples were coded with patient identifiers removed.

Animals and surgical models

Wild-type C57BL/6J mice were purchased from the Jackson Laboratory (Bar Harbor, ME). *Nrf2*^{-/-} mice on C57BL background were obtained from the Experimental Animal Division, RIKEN Biosource Center (Tsukuba, Japan). All animal experiments were approved by the Institutional Animal Care and Use Committees at North Carolina Central University (protocol number XC-12-03-2008).

Eight-week-old wild-type and *Nrf2*^{-/-} mice were housed five per cage respectively, given a diet and water *ad libitum* and maintained on a 12h light-dark cycle. These mice were administered anesthetics pre-mixed in normal saline (80mg/kg ketamine and 12mg/kg xylazine, *i.p.*). All surgeries were performed through an upper midline incision. (1) Esophagogastric anastomosis (Figure 2A): Three incisions of ~5 mm were made on the distal esophagus and the forestomach, and then sutured longitudinally with accurate mucosal to mucosal opposition, for example, point *a* with *b*, point *c* with *d*. (2) Esophagogastrroduodenal anastomosis (Figure 2B): Two 5-mm incisions were made on the esophagus and the duodenum, and then anastomosed together with accurate mucosal to mucosal opposition. (3) Esophagogastrroduodenal anastomosis plus gastrectomy (Figure 2C): In addition to esophagogastrroduodenal anastomosis, the stomach was removed after ligating at the gastroesophageal junction and the pylorus. After anastomoses, the abdominal cavity was washed and closed with 6-0 silk suture. Esophagogastric anastomosis was designed to eliminate the sphincter function and allow free gastric reflux, whereas esophagogastrroduodenal anastomosis plus gastrectomy and esophagogastrroduodenal anastomosis were for duodenal reflux and mixed reflux, respectively.

Transepithelial electrical resistance (TEER)

Esophageal epithelial tissues for chamber studies were immersed in ice-cold oxygenated Ringer's solution and immediately transported to the laboratory for mounting mucosal side up in mini-Ussing chambers as previously described⁹. After equilibration for 30 min, basal electrical readings of PD, *I*_{sc}, and *R*_T were obtained every 15 min for two hours. Total electrical resistance (*R*_T) was calculated using Ohm's law, where $PD = I_{sc} \times R_T$.

Transmission electron microscopy (TEM)

Three mice of each group were sacrificed and the esophageal epithelial tissues were dissected. The tissue was fixed with 4% glutaraldehyde in cacodylate buffer for at least one hour and then washed in buffer and postfixed for 1 hr in 1% OsO₄ in the same buffer. It was washed in veronal acetate buffer, stained for 1 hr in 0.5 uranyl acetate in the same buffer, dehydrated using a graded ethanol series, and embedded in Poly/Bed 812 resin (Polysciences Warrington, PA). Thick and thin sections were prepared on a Reichert-Jung ultramicrotome (Leica, Bannockburn, IL). Thick sections (0.5 micrometer) on slides were stained with 1% toluidine blue-borax for light microscopy selection of the appropriate areas for thin sections; thin sections were mounted on copper grids and double stained with 2% uranyl acetate and Reynolds' lead citrate. The grids were examined using a Philips CM 12 electron microscope (FEI, Hillsboro, OR). From each sample, intercellular space (ICS) and

density of electron-dense material between >30 randomly selected basal cells were measured on three photomicrographs with the MicroSuite Biological Suite (Olympus, Center Valley, PA). At least ten randomly selected cells were used for the measurement. The ICS was measured as the area between cell membrane of two adjacent cells. Density of electron-dense material in ICS was calculated as the average gray value divided by ICS. ANOVA test was performed to compare the differences between groups.

RNA isolation and microarray analysis

Three mice of each group were sacrificed and the esophageal epitheliums were dissected. Total RNA was extracted from individual mouse esophagi with an RNeasy Fibrous Tissue Mini Kit (Qiagen, Valencia, CA). These RNA samples were checked for their quality using gel electrophoresis and their concentrations were measured using spectrophotometry. RNA quality (RIN>7) was further checked with Bioanalyzer (Agilent Technologies, Santa Clara, CA).

Microarray experiments with mouse samples were performed with Agilent two-channel mouse 4×44k microarrays in the Genomics Core of University of North Carolina at Chapel Hill. Data preprocessing was carried out via UNC Microarray Database for quality filtering and data normalization. The retrieved matrix data was collapsed onto Gene symbol as the gene expression value. Differentially expressed genes (DEGs) were obtained from two-class SAM in Excel with the median number of false positives less than 1. GSA was carried out as an add-in in Excel. Curated gene sets in two major categories - canonical pathway (CP; 880 gene sets) and Gene Ontology (GO; C5, 1,454 gene sets) - were downloaded from the GSEA web portal and used in this study (<http://www.broadinstitute.org/gsea/index.jsp>). 1000 permutations were applied to generate a null distribution for statistical testing, and significantly enriched gene sets were obtained at a false discovery rate (FDR) cutoff of 0.5. The microarray data were submitted to the GEO database (GSE39629).

Western blotting

Two 3-month-old mice were sacrificed and the esophageal epitheliums were dissected. Total proteins were isolated from the individual esophageal epithelium, tongue tissue and liver tissue by an adaptation of a previously described method.⁹ Protein concentration was determined by the BCA protein assay (Pierce; Rockford, IL). Protein samples were separated by PAGE, and transferred to a PVDF membrane. After blocking with 0.5% non-fat dry milk, the membrane was probed with a rabbit anti-Claudin-1 polyclonal antibody diluted at 1: 50 (LS-B6327, Cell Signaling Technology, Danvers, MA), a rabbit anti-Claudin-4 polyclonal antibody diluted at 1: 25 (LS-B2370, Cell Signaling Technology) or 3 µg/ml mouse anti-Cox IV monoclonal antibody (ab14744, Abcam; Cambridge, MA) at 4°C overnight. We use 0.4 µg/ml rabbit anti-Nrf2 polyclonal antibody (H-300, Santa Cruz Biotechnology, Santa Cruz, CA) for confirmation of the absence of Nrf2 protein in the esophageal epithelium of Nrf2^{-/-} mice (Figure S2). The membrane was then incubated with HRP-conjugated anti-mouse or anti-rabbit secondary antibody. Immunoreactivity was visualized by applying HRP ECL substrate (Pierce) and immediately exposing the membranes to X-ray film. To verify equal loading of samples, the blots were stripped and re-probed with mouse anti-β-actin monoclonal antibody diluted at 1:2500 (A-5441, Sigma-Aldrich; St. Louis, MO).

Histochemical and immunohistochemical staining

Tissues were routinely processed for paraffin sectioning (5µm). HE staining was carried out with standard protocols. The thickness of the keratinized layer was measured on HE stained sections using MicroSuite Biological Suite. For immunohistochemical staining, the deparaffinized sections were submerged in methanol containing 0.3% hydrogen peroxide for

15 min at RT to inhibit endogenous peroxidase activity. Antigen retrieval was done prior to incubation with 1:100 diluted rabbit anti-Nrf2 polyclonal antibody (PA1-38312, Thermo Scientific, Rockford, IL), 1:50 diluted rabbit anti-HO1 polyclonal antibody (ab52947, Abcam), 5 µg/ml rabbit anti-Claudin 1 polyclonal antibody (51-9000, Invitrogen), 10 µg/ml mouse anti-Claudin 4 monoclonal antibody (32-9400, Invitrogen), or 1.25 µg/ml mouse anti-8OHdG monoclonal antibody (ab48508; Abcam) overnight at 4°C. We use anti-Keratin 5 antibody () as standard control for IHC (Figure S3), Tissue sections were then washed again in PBS and incubated with peroxidase-conjugated secondary antibodies for 30 minutes at 37°C. Detection of the antibody complex was done using the streptavidin-peroxidase reaction kit with DAB as a chromogen (ABC kit, Vector Labs; Burlingame, CA).

The percentage of Nrf2 positive cells/total cells and cells with nuclear staining/total positive cells on the 10 human samples of normal and GERD, and 3 mouse samples of NOC, gastric, duodenal and mixed reflux model were calculated and statistically analyzed. The percentage of positively stained cells was measured in three wild-type and three Nrf2^{-/-} mice. Three sections were used for each sample. Statistical analysis was performed to compare the expression level of 8OHdG in wild-type and Nrf2^{-/-} mice.

Measurement of ATP concentration

Esophageal epithelial tissue samples were weighed and homogenized in 400 µl 5% TCA. The supernatant was diluted 1:10 with distilled water for ATP measurement using a bioluminescence ATP assay kit according to the manufacturer's instructions (EnzyLight ATP assay kit; BioAssay Systems; Hayward, CA). The luminescence signal was measured within 3 min using the ATP luminometry mode in a plate reader (Wallac Victor3; PerkinElmer; Hanover, MD) with an integration time of 1.0 s and calibrated to a standard curve. The concentration of ATP was calculated by dividing the total amount by the weight of each sample.

Chromatin immunoprecipitation (ChIP)

Nrf2 binding sites within the 5kb 5'-upstream DNA sequence of Cldn4 (ENSMUSG00000047501) were predicted using Anchored Combination TFBS Cluster Analysis (oPOSSUM version 3.0).¹⁰ The "Conserved Binding Site Cluster Combinations" (TGAGTCA) were found at -341bp ~ -347bp and -423bp ~ -429bp upstream of Cldn4. ChIP analysis was performed in triplicate using an EZ-ChIP kit (Millipore; Billerica, MA) according to the manufacturer's instructions. Immunoprecipitations were performed using control mouse IgG or 2 µg/ml rabbit anti-Nrf2 polyclonal antibody (H-300, Santa Cruz Biotechnology). Two µl of the immunoprecipitated DNA or input was used for 35 cycles of PCR with the following primer pairs: Cldn4 (5'-GTTGTCCCCACCCGGTGAGCATC-3' and 5'-GGCCAACAAAGGCGTTCAGAGGC-3'; predicted size: 168 bp); Nqo1 (5'-GCAGTTTCTAAGAGCAGAACG-3' and 5'-GTAGATTAGTCCTCACTCAGCCG-3'; predicted size: 176 bp); P63 (5'-CAAATGTTGCTTGCTGTGGTG-3' and 5'-GTCAGTCGAGTGCACAGTTT-3'; predicted size: 210 bp). As a known Nrf2 target gene, Nqo1 serves as a positive control, and P63 as a negative control.

RESULTS

Activation of Nrf2 in esophageal epithelial cells by gastroesophageal reflux

Nrf2 expression was examined in ten human biopsy samples of normal esophagus and GERD. In normal esophagus (Figure 1A), Nrf2 protein was detected mostly in the cytoplasm of superficial cells (Figure 1C), but not in basal cells (Figure 1E). However, in GERD biopsies (Figure 1B), immunostaining showed overexpression and nuclear localization of Nrf2 in superficial cells (Figure 1D) and basal cells (Figure 1F). The number

of cells was counted, the percentages were calculated and the statistical significances were analyzed. The positive stained cells were $18.2 \pm 1.8\%$ of the total cells in normal esophageal epithelium and $39.7 \pm 7.6\%$ in GERD. Statistical analysis showed the up-regulation of Nrf2 protein in GERD was significant ($P < 0.05$) (Figure 1I). The cells with nuclear staining were $8.7 \pm 1.9\%$ of the total positive cells in normal esophageal epithelium and $93.3 \pm 11.6\%$ in GERD. Statistical analysis showed the amount of Nrf2 protein in nuclear is significantly higher in GERD ($P < 0.001$) (Figure 1J). The expression of HO1, a canonical Nrf2 target gene, was also examined by immunohistochemistry. The result showed HO1 was up-regulated in GERD (Figure 1G, H). These data suggested that, as an integral part of the molecular network in normal esophageal epithelial cells, Nrf2 was activated by gastroesophageal reflux.

To further investigate the involvement of Nrf2 in GERD, three surgical mouse models were developed to produce gastric reflux (Figure 2A), duodenal reflux (Figure 2B), or mixed reflux (Figure 2C). Three mice of each group were used for further experiments. In normal mouse esophageal epithelium, Nrf2 protein was localized in the cytoplasm of superficial and parabasal cells. Nuclear localization was observed in superficial, parabasal and basal cells 4 weeks after gastric reflux (Figure 2E), duodenal reflux (Figure 2F), or mixed reflux (Figure 2G). The positively stained cells were $23.9 \pm 4.1\%$ of the total epithelial cells in control mice, $54.2 \pm 5.1\%$ in gastric reflux ($P < 0.001$), $72.1 \pm 4.3\%$ in duodenal reflux ($P < 0.001$), and $35.6 \pm 5.8\%$ in mixed reflux ($P < 0.001$; as compared to the control) (Figure 2H). Positive cells with nuclear staining were $27.9 \pm 2.1\%$ of the positively stained cells in control mice, $66.3 \pm 7.3\%$ in gastric reflux ($P < 0.001$), $89.7 \pm 2.9\%$ in duodenal reflux ($P < 0.001$), and $63.3 \pm 1.3\%$ in mixed reflux ($P < 0.001$; as compared to the control) (Figure 2I). The expression of HO1, a canonical Nrf2 target gene, was also examined by immunohistochemistry (Figure 2J, K, L, M). The result showed HO1 was up-regulated in mouse model of duodenal reflux and mixed reflux (Figure 2L, M). These results confirmed Nrf2 activation during gastroesophageal reflux in mice, and prompted us to further study the role of Nrf2 in the esophagus using these models.

Impaired barrier function of the esophageal epithelium in Nrf2^{-/-} mice

As an indicator of barrier function, TEER of esophageal epithelium in Nrf2^{-/-} mice was significantly lower than that in wild-type mice at each time point (Figure 3A), suggesting a protective role of Nrf2 against ion transport in esophageal epithelium. We further measured TEER of esophageal epithelium in wild-type and Nrf2^{-/-} mice 4 weeks after reflux surgery. Significant decrease in esophageal TEER was observed in both wild-type and Nrf2^{-/-} mice after gastroesophageal reflux, especially in those with gastric or duodenal reflux (Figure 3B). - Nrf2 deficiency further reduced esophageal TEER after gastric or mixed reflux ($P < 0.01$), but not after duodenal reflux. Dramatic decrease of TEER after duodenal reflux overshadowed the effect of Nrf2 deficiency. These data demonstrated a protective role of Nrf2 in epithelial resistance both in the presence and absence of gastroesophageal reflux.

Histological and ultrastructural changes in the esophageal epithelium of Nrf2^{-/-} mice

In order to understand the structural basis of Nrf2 function in esophageal epithelium, esophageal tissue sections of wild-type and Nrf2^{-/-} mice were compared. On HE-stained sections, no obvious histological changes could be observed in the esophageal epithelium of Nrf2^{-/-} mice as compared with wild-type mice (Figure S1A, B). Since a previous study suggested Nrf2 deficiency impacted the cornification of esophageal epithelium,¹¹ we measured the thickness of esophageal epithelium in wild-type and Nrf2^{-/-} mice. However, we did not observe any difference between wild-type and Nrf2^{-/-} mice (Figure S1C).

Under TEM, dilated intercellular spaces (DIS) and a decrease of the number of mitochondria were observed in the basal layer of the esophagus from Nrf2^{-/-} mice (Figure 4E), as compared to wild-type (Figure 4A). In Nrf2^{-/-} samples, there were fewer visible desmosomes and less electron-dense materials between basal cells (Figure 4E), suggesting weakened cell-cell adhesion between basal cells in Nrf2^{-/-} mice. There were also fewer cellular processes extending from basal cells into basal lamina in Nrf2^{-/-} mice (Figure 4E), suggesting weakened cell-matrix adhesion in Nrf2^{-/-} mice.

After exposure to reflux for 4 weeks, DIS was observed in the basal layer of esophageal epithelium of wild-type mice (Figure 4B, C, D). Nrf2 deficiency aggravated these ultrastructural changes in esophageal epithelial of Nrf2^{-/-} mice (Figure 4F, G, H). This was especially obvious in the case of gastric reflux (Figure 4B and 4F). Quantitative analysis confirmed a significant increase of intercellular space between basal cells of Nrf2^{-/-} mice as compared to wild-type (Figure S4A), and a significant decrease of electron-dense materials (Figure S4B). This tendency was especially significant in the presence of gastric reflux.

Differentially expressed genes and gene sets in esophageal epithelium of wild-type and Nrf2^{-/-} mice

To further understand the molecular mechanism of impaired esophageal barrier function in Nrf2^{-/-} mice, gene expression microarray was performed on wild-type and Nrf2^{-/-} esophageal epithelial samples (three of each group). SAM analysis revealed that 15 known Nrf2 target genes (Akr1b8, Gclc, Gsta3, Gstm1, Gstm3, Nfe2l2, Nqo1, Ahsg, Ces1, Esd, Gstp1, Mgst1, Npn3, Pparg and Selenbp2) were down-regulated in Nrf2^{-/-} mice as compared with wild-type mice (Suppl. Excel 1). Since these genes are known to be associated with stress response and detoxification, our data suggest that Nrf2 is normally activated in the esophageal epithelium of wild-type mice in order to provide protection against physiological stress.

In the presence of gastric reflux, 7 known Nrf2 target genes (Nqo1, Gstm1, Akr1b8, Gstm3, Gclc, Pln, Gstp1) were down-regulated in Nrf2^{-/-} mice as compared to wild-type. In the presence of duodenal reflux, 5 known Nrf2 target genes (Nfe2l2, Nqo1, Gstm1, Gstm3, Ptgr1) were down-regulated. In the presence of mixed reflux, 24 known Nrf2 target genes (Gstm1, Gsta3, Gstm3, Nfe2l2, Nqo1, Gstm2, Blvr, Hmox1, Entpd5, Cbr3, Ppp1r12b, Gclc, Mgst3, Gstm5, Txnrd1, Cat, Meis1, Ftl1, Sdpr, Selenbp2, Pparg, Gstp1, Esd, Mgst1) were down-regulated (Suppl. Excel 1).

We also analyzed array data to identify differentially expressed gene sets with GSA. Twenty gene sets related to response to stimulus/stress and oxidoreductase activity were down-regulated in the esophageal epithelium of Nrf2^{-/-} mice as compared with wild-type mice. Consistent with the observation of fewer mitochondria in the basal cells of Nrf2^{-/-} mice, 11 gene sets associated with mitochondrial biogenesis and 32 gene sets associated with metabolism and energy were down-regulated in the esophageal epithelium of Nrf2^{-/-} mice (Suppl. Excel 2).

Increased oxidative damage and mitochondrial dysfunction in the esophageal epithelium of Nrf2^{-/-} mice

Since Nrf2 deficiency resulted in down-regulation of response to stimulus/stress and oxidoreductase activity, we examined the level of 8OHdG, an oxidative DNA damage marker, in the esophageal epithelium with immunostaining. It was clear that 8OHdG dramatically increased in the nuclei of the esophageal epithelial cells in Nrf2^{-/-} mice as compared to wild-type (Figure 5A, B, A', B'). The percentage of 8OHdG positive cells

significantly increased in Nrf2^{-/-} mice (47.5±3.0%) as compared with wild-type mice (9.4±1.8%) (P<0.001) (Figure 5E).

We also measured ATP concentration and expression of a mitochondrial marker protein (Cox IV) in the esophageal epithelium. ATP concentration decreased significantly in the esophageal epithelium of Nrf2^{-/-} mice as compared to wild-type (Figure 5D). Meanwhile, down-regulation of Cox IV was detected with Western blotting (Figure 5C), and quantification analysis showed significant decrease of Cox IV protein in Nrf2^{-/-} mice (Figure 5 F). These results suggested mitochondrial dysfunction in the esophageal epithelium of Nrf2^{-/-} mice.

Down-regulation of Cldn4 in the esophageal epithelium of Nrf2^{-/-} mice

The tight junction is the most important barrier in epithelial tissues, and a key protein constituent of the tight junction is transmembrane claudins (Cldn).¹² Of 24 family members, Claudin 4 (Cldn4) and Claudin 1 (Cldn1) are the dominant ones in normal esophageal epithelium.⁹ Therefore, we examined the expression of Cldn4 and Cldn1 in the esophageal epithelium of mice.

Immunostaining showed Cldn4 expression in the cytoplasm and cell membrane of esophageal epithelial cells of wild-type mice (Figure 6A), and its down-regulation in Nrf2^{-/-} mice (Figure 6C). Western blotting confirmed down-regulation of Cldn4 by 33% in the esophageal epithelium of Nrf2^{-/-} mice as compared with wild-type mice (Figure 6E). No obvious change of Cldn1 expression was observed in Nrf2^{-/-} mice (Figure 6B, D).

Nrf2 binding sites within the 5kb 5'-upstream DNA sequence of Cldn4 (ENSMUSG00000047501) were predicted using Anchored Combination TFBS Cluster Analysis (oPOSSUM version 3.0).¹⁰ The "Conserved Binding Site Cluster Combinations" (TGAGTCA) were found at -341bp ~ -347bp and -423bp ~ -429bp upstream of Cldn4. Using Anchored Combination TFBS Cluster Analysis (oPOSSUM version 3.0) we also analyzed 5,000-bp upstream DNA sequence of murine Cldn1 for potential Nrf2 binding sites. Absence of such sites explains why Nrf2^{-/-} mice expressed the same amount of Cldn1 as wild-type mice.

ChIP analysis confirmed the direct binding of Nrf2 on the predicted AREs of Cldn4 (Figure 6F) in the esophageal epithelium of both non-operated mice and the duodenal reflux model. Nrf2 binding to Nqo1 was also detected by ChIP as a positive control of Nrf2 target gene. Contamination of genomic DNA was controlled by amplification of a 210 bp segment of P63 gene which is not bound by Nrf2.

DISCUSSION

This study is the first to demonstrate a critical role of Nrf2 in esophageal barrier function. With three surgical models of GERD in mice, we demonstrated that gastroesophageal reflux activated Nrf2 as a defense mechanism. Our data suggested that Nrf2 deficiency impaired the energy-dependent tight junctions in the esophageal epithelium through mitochondrial dysfunction and Cldn4 down-regulation.

Gastroesophageal reflux is known to produce oxidative stress in the esophageal epithelium.¹³ Oxidative damage has long been proposed as one of the mechanisms for GERD, Barrett's esophagus and adenocarcinoma.¹⁴ As a major cellular defense mechanism against oxidative stress, the Nrf2/Keap1 pathway regulates expression of enzymes involved in detoxification and anti-oxidative stress response.³ Using human samples and mouse surgical models, we found Nrf2 was activated in GERD as evidenced by its nuclear

localization and overexpression (Figure 2). Consistent with our observations, previous studies on rat models of GERD also showed up-regulation of Nrf2 target genes, such as HO1, MT1.¹⁵¹⁶

Since oxidative stress is known to impair the epithelial barrier function in the gut, the stomach and the trachea,¹⁷¹⁸¹⁹ we studied the role of Nrf2 in esophageal barrier function using wild-type and knockout mice. Nrf2 deficiency clearly reduced TEER without reflux (Figure 3A), suggesting a baseline protection by Nrf2 under physiological conditions. In mice models of GERD, Nrf2 also showed a protective function, especially in the presence of gastric or mixed reflux. Nrf2 deficiency further reduced TEER that had been suppressed by reflux (Figure 3B). This is consistent with previous work suggesting that gastroesophageal reflux produced reactive oxygen species, induced DIS, and impaired the barrier function of esophageal epithelium.^{20, 21, 22}

In order to understand how Nrf2 may regulate the barrier function of esophageal epithelium, we investigated the impact of Nrf2 deficiency on epithelial structure. Microscopically, no obvious change of cornification was observed on the esophageal epithelium of Nrf2^{-/-} mice (Figure S1). Under TEM, we noticed DIS and a reduction of mitochondria in the esophageal epithelium of Nrf2^{-/-} mice as compared with wild-type (Figure 4). Consistent with this observation, mitochondrion-related gene sets were down-regulated in the esophageal epithelium of Nrf2^{-/-} mice (Excel S2), and oxidative DNA damage increased in the epithelial cells of Nrf2^{-/-} mice (Figure 5A, B). Reduction of mitochondria was confirmed by down-regulation of a mitochondrial marker protein, Cox IV (Figure 5D). Our data were in agreement with previous studies showing that Nrf2 regulates mitochondrial biogenesis,²³ and oxidative stress impairs mitochondrial biogenesis.²⁴ In fact, mitochondrial dysfunction and ATP depletion are known to impact the formation and function of tight junctions.^{17, 252627} However, it is still unclear how Nrf2 deficiency may cause mitochondrial dysfunction, although Keap1 and Nrf2 have been shown to be tethered to mitochondria through PGAM5 and p62.²⁸²⁹

The tight junction is known to be the most important structure for epithelial barrier function,³⁰ and claudins are key tight junction proteins that regulate solute movement across polarized epithelia.¹² We compared expression of Cldn1 and Cldn4 between the esophageal epithelium of wild-type and Nrf2^{-/-} mice, because these two are the major claudins in normal esophageal epithelium.⁹ Both immunostaining and Western blotting showed significant down-regulation of Cldn4, but not Cldn1, in the esophageal epithelium of Nrf2^{-/-} mice. ChIP analysis clearly showed binding of Nrf2 to the predicted AREs in the promoter region of mouse Cldn4 gene (Figure 6). These data are consistent with previous studies in the literature. *In vitro* experiments have shown that acid, bile salts, and acidic bile salts modulated the barrier function of epithelial cells by altering the expression and localization of Cldn4.³¹³²³³ ChIP-seq experiments have showed that Nrf2 binds the ARE motif of Cldn3 in human lymphoblastoid cells and Cldn4 in mouse embryonic fibroblasts.³⁴³⁵ Sulforaphane, an Nrf2 activator, significantly increased Cldn5 expression and thus protected the blood-brain barrier after brain injury.³⁶ Quercetin, another Nrf2 activator,³⁷ enhanced intestinal barrier function through up-regulation of Cldn4 in Caco-2 cells.^{38, 3940} In summary, our data suggested that Nrf2 deficiency caused mitochondrial dysfunction, down-regulated Cldn4, and ultimately impaired energy-dependent tight junction in the esophageal epithelium.

This study focused on comparison between Nrf2^{-/-} and wild-type mice. We did not further look into mitochondrial dysfunction, oxidative damage and Cldn expression in all three reflux models. These studies need to be done in the future in order to understand how

gastroesophageal reflux impairs esophageal barrier function. It is also interesting how Nrf2 may interact with reflux in modulating the barrier function.

Nrf2 activators have been used in clinical trials for human diseases associated with oxidative stress such as cancer and chronic kidney disease.⁴¹⁴² However, whether Nrf2 interacts with different refluxes is still unclear. Further study will be done to determine the involvement of Nrf2 in the three mouse models of GERD.

It should be noted that mouse esophagus is lined by a fully keratinized epithelium that is more sensitive to duodenal refluxate than to gastric refluxate. Gastric reflux in mouse esophagus does not produce evident inflammation, unlike gastric acid exposure in the rabbit model and human patients. Because of these differences between mouse and human esophagus, mouse models have limitations and further studies are needed before mouse data can be translated into human studies.

Our study has potentially significant clinical implications: Nrf2 activators may strengthen the barrier function of esophageal epithelium. As many as 10-40% of patients find their symptoms inadequately controlled by PPI, especially at night.⁴³ It remains a clinical challenge to manage PPI failures.⁴⁴⁴⁵ Nrf2 activators might be an additional pharmaceutical option to augment the existing treatment modalities. Also, recently radiofrequency ablation has been established as an effective and safe treatment for Barrett's with dysplasia.⁴⁶⁴⁷ Ablation restores an endoscopically normal neosquamous epithelium, which is usually histologically similar to normal esophageal squamous epithelium and does not possess the molecular alterations characteristic of Barrett's epithelium.⁴⁸⁴⁹ However, oxidative stress remains high after ablation, as evidenced by higher levels of 8OHdG and SOD activity.⁵⁰ Functionally, the barrier function of the neosquamous epithelium is sub-optimal; its electrical resistance has been demonstrated to be significantly lower than that of normal esophagus, and equivalent to GERD.⁵¹ Therefore, strengthening the neo-squamous epithelium with an Nrf2 activator may be a potential solution.

Regardless of these potential treatment ramifications, our observations have implications for understanding the pathogenesis of GERD. It has long been known that some subjects tolerate high levels of intra-esophageal acid exposure without developing signs or symptoms of GERD, while others will manifest severe erosive esophagitis or precancerous lesions at relatively low levels of acid exposure. Clearly, host factors must play an important role in GERD susceptibility. However, these factors are poorly understood. If the function of the Nrf2/Keap1 pathway is integral to mucosal integrity, variability in its function may at least partially explain the heterogeneous manifestations of GERD. Indeed, genetic polymorphism of GSTP1, a known Nrf2 target gene, is correlated with a higher grade of esophagitis.⁵² While our work suggests this intriguing possibility, further investigation will be essential to establish this pathway as an integral predictor of disease or target for therapies.

In conclusion, our study first demonstrates that Nrf2 deficiency impairs esophageal barrier function through disrupting energy-dependent tight junction. Elucidating the role of this pathway in GERD has potential implications for the pathogenesis and therapy of the disease.

Supplementary Material

Refer to Web version on PubMed Central for supplementary material.

Acknowledgments

The authors acknowledge excellent microarray service by Dr. Yan Shi and her staff at the Genomics Core Facility, Lineberger Comprehensive Cancer Center, University of North Carolina at Chapel Hill, Chapel Hill, NC. The

authors also thank Dr. Sara E. Miller and Mr. Phillip Christopher at the Department of Pathology, Duke University, Durham, NC, for their excellent electron microscopy service.

FUNDING NIH U54 CA156735 and Takeda MA-NC-D-156.

Abbreviations

ARE	antioxidant response element
Cldn	claudin
ChIP	chromatin immunoprecipitation
CP	canonical pathway
DEG	differentially expressed gene
DIS	dilated intercellular space
FDR	false discovery rate
GERD	gastroesophageal reflux disease
GO	gene ontology
GSA	gene set analysis
ICS	intercellular space
Keap1	Kelch-like ECH-associated protein 1
Nrf2 (or Nfe2l2)	nuclear factor erythroid derived 2 like 2
R_T	total electrical resistance
TEER	trans-epithelial electrical resistance
TEM	transmission electron microscopy

REFERENCES

1. Orlando LA, Orlando RC. Pathophysiology of GERD: Esophageal Epithelial Defense. *Practical Gastroenterology*. 2004;16–57.
2. Orlando RC. The integrity of the esophageal mucosa. Balance between offensive and defensive mechanisms. *Best Pract Res Clin Gastroenterol*. 2010; 24:873–82. [PubMed: 21126700]
3. Kensler TW, Wakabayashi N, Biswal S. Cell survival responses to environmental stresses via the Keap1-Nrf2-ARE pathway. *Annu Rev Pharmacol Toxicol*. 2007; 47:89–116. [PubMed: 16968214]
4. Suzuki T, Maher J, Yamamoto M. Select heterozygous Keap1 mutations have a dominant-negative effect on wild-type Keap1 in vivo. *Cancer Res*. 2011; 71:1700–9. [PubMed: 21177379]
5. Wakabayashi N, et al. Keap1-null mutation leads to postnatal lethality due to constitutive Nrf2 activation. *Nat Genet*. 2003; 35:238–45. [PubMed: 14517554]
6. Chen H, et al. Transcript profiling identifies dynamic gene expression patterns and an important role for Nrf2/Keap1 pathway in the developing mouse esophagus. *PLoS One*. 2012; 7:e36504. [PubMed: 22567161]
7. Simpson CL, Patel DM, Green KJ. Deconstructing the skin: cytoarchitectural determinants of epidermal morphogenesis. *Nat Rev Mol Cell Biol*. 2011; 12:565–80. [PubMed: 21860392]
8. Vermeij WP, Alia A, Backendorf C. ROS quenching potential of the epidermal cornified cell envelope. *J Invest Dermatol*. 2011; 131:1435–41. [PubMed: 21248766]
9. Jovov B, et al. Claudin-18: a dominant tight junction protein in Barrett's esophagus and likely contributor to its acid resistance. *Am J Physiol Gastrointest Liver Physiol*. 2007; 293:G1106–13. [PubMed: 17932229]

10. Ho Sui SJ, et al. oPOSSUM: identification of over-represented transcription factor binding sites in co-expressed genes. *Nucleic Acids Res.* 2005; 33:3154–64. [PubMed: 15933209]
11. Wruck CJ, et al. Impact of Nrf2 on esophagus epithelium cornification. *Int J Dermatol.* 2011; 50:1362–5. [PubMed: 22004488]
12. Overgaard CE, et al. Claudins: control of barrier function and regulation in response to oxidant stress. *Antioxid Redox Signal.* 2011; 15:1179–93. [PubMed: 21275791]
13. Yoshida N. Inflammation and oxidative stress in gastroesophageal reflux disease. *J Clin Biochem Nutr.* 2007; 40:13–23. [PubMed: 18437209]
14. Chen X, Yang CS. Esophageal adenocarcinoma: a review and perspectives on the mechanism of carcinogenesis and chemoprevention. *Carcinogenesis.* 2001; 22:1119–29. [PubMed: 11470739]
15. Chen X, et al. Oxidative damage in an esophageal adenocarcinoma model with rats. *Carcinogenesis.* 2000; 21:257–63. [PubMed: 10657966]
16. Kruel CR, et al. Evaluation of the heme oxygenase-1 expression in esophagitis and esophageal cancer induced by different reflux experimental models and diethylnitrosamine. *Acta Cir Bras.* 2010; 25:304–10. [PubMed: 20498946]
17. Lewis K, McKay DM. Metabolic stress evokes decreases in epithelial barrier function. *Ann N Y Acad Sci.* 2009; 1165:327–37. [PubMed: 19538324]
18. Hashimoto K, et al. Oxidative stress induces gastric epithelial permeability through claudin-3. *Biochem Biophys Res Commun.* 2008; 376:154–7. [PubMed: 18774778]
19. Morrison D, et al. Epithelial permeability, inflammation, and oxidant stress in the air spaces of smokers. *Am J Respir Crit Care Med.* 1999; 159:473–9. [PubMed: 9927360]
20. Ito H, et al. Reactive nitrogen oxide species induce dilatation of the intercellular space of rat esophagus. *Scand J Gastroenterol.* 2010; 45:282–91. [PubMed: 20001645]
21. Lin BR, et al. Luminal hydrochloric acid stimulates rapid transepithelial ion fluxes in rodent esophageal stratified squamous epithelium. *J Physiol Pharmacol.* 2008; 59:525–42. [PubMed: 18953095]
22. Farre R, et al. Acid and weakly acidic solutions impair mucosal integrity of distal exposed and proximal non-exposed human oesophagus. *Gut.* 2010; 59:164–9. [PubMed: 19880965]
23. Piantadosi CA, et al. Heme oxygenase-1 regulates cardiac mitochondrial biogenesis via Nrf2-mediated transcriptional control of nuclear respiratory factor-1. *Circ Res.* 2008; 103:1232–40. [PubMed: 18845810]
24. Wu CW, et al. Enhanced oxidative stress and aberrant mitochondrial biogenesis in human neuroblastoma SH-SY5Y cells during methamphetamine induced apoptosis. *Toxicol Appl Pharmacol.* 2007; 220:243–51. [PubMed: 17350664]
25. Madsen KL, et al. FK506 increases permeability in rat intestine by inhibiting mitochondrial function. *Gastroenterology.* 1995; 109:107–14. [PubMed: 7540994]
26. Bacallao R, et al. ATP depletion: a novel method to study junctional properties in epithelial tissues. I. Rearrangement of the actin cytoskeleton. *J Cell Sci.* 1994; 107:3301–13. [PubMed: 7706387]
27. Mandel LJ, Doctor RB, Bacallao R. ATP depletion: a novel method to study junctional properties in epithelial tissues. II. Internalization of Na⁺,K⁺-ATPase and E-cadherin. *J Cell Sci.* 1994; 107:3315–24. [PubMed: 7706388]
28. Lo SC, Hannink M. PGAM5 tethers a ternary complex containing Keap1 and Nrf2 to mitochondria. *Exp Cell Res.* 2008; 314:1789–803. [PubMed: 18387606]
29. Kwon J, et al. Assurance of mitochondrial integrity and mammalian longevity by the p62-Keap1-Nrf2-Nqo1 cascade. *EMBO Rep.* 2012; 13:150–6. [PubMed: 22222206]
30. Blasig IE, Haseloff RF. Tight junctions and tissue barriers. *Antioxid Redox Signal.* 2011; 15:1163–6. [PubMed: 21446883]
31. Oshima T, et al. Acid modulates the squamous epithelial barrier function by modulating the localization of claudins in the superficial layers. *Lab Invest.* 2012; 92:22–31. [PubMed: 21912379]
32. Chen X, et al. Acidic bile salts modulate the squamous epithelial barrier function by modulating tight junction proteins. *Am J Physiol Gastrointest Liver Physiol.* 2011; 301:G203–9. [PubMed: 21617116]

33. Chen X, et al. Bile salts disrupt human esophageal squamous epithelial barrier function by modulating tight junction proteins. *Am J Physiol Gastrointest Liver Physiol*. 2012; 303:G199–208. [PubMed: 22575221]
34. Chorley BN, et al. Identification of novel NRF2-regulated genes by ChIP-Seq: influence on retinoid X receptor alpha. *Nucleic Acids Res*. 2012 [Epub ahead of print].
35. Malhotra D, et al. Global mapping of binding sites for Nrf2 identifies novel targets in cell survival response through ChIP-Seq profiling and network analysis. *Nucleic Acids Res*. 2010; 38:5718–34. [PubMed: 20460467]
36. Zhao J, et al. Enhancing expression of Nrf2-driven genes protects the blood brain barrier after brain injury. *J Neurosci*. 2007; 27:10240–8. [PubMed: 17881530]
37. Arredondo F, et al. After cellular internalization, quercetin causes Nrf2 nuclear translocation, increases glutathione levels, and prevents neuronal death against an oxidative insult. *Free Radic Biol Med*. 2010; 49:738–47. [PubMed: 20554019]
38. Amasheh M, et al. Quercetin enhances epithelial barrier function and increases claudin-4 expression in Caco-2 cells. *J Nutr*. 2008; 138:1067–73. [PubMed: 18492835]
39. Suzuki T, Hara H. Quercetin enhances intestinal barrier function through the assembly of zonula [corrected] occludens-2, occludin, and claudin-1 and the expression of claudin-4 in Caco-2 cells. *J Nutr*. 2009; 139:965–74. [PubMed: 19297429]
40. Rao CV, Vijayakumar M. Effect of quercetin, flavonoids and alpha-tocopherol, an antioxidant vitamin, on experimental reflux oesophagitis in rats. *Eur J Pharmacol*. 2008; 589:233–8. [PubMed: 18547560]
41. Egner PA, et al. Bioavailability of Sulforaphane from two broccoli sprout beverages: results of a short-term, cross-over clinical trial in Qidong, China. *Cancer Prev Res (Phila)*. 2011; 4:384–95. [PubMed: 21372038]
42. Pergola PE, et al. Bardoxolone methyl and kidney function in CKD with type 2 diabetes. *N Engl J Med*. 2011; 365:327–36. [PubMed: 21699484]
43. Hershcovici T, Fass R. Management of gastroesophageal reflux disease that does not respond well to proton pump inhibitors. *Curr Opin Gastroenterol*. 2010; 26:367–78. [PubMed: 20571388]
44. Ang D, Sifrim D, Tack J. Mechanisms of heartburn. *Nat Clin Pract Gastroenterol Hepatol*. 2008; 5:383–92. [PubMed: 18542113]
45. Yuan Y, Hunt RH. Evolving issues in the management of reflux disease? *Curr Opin Gastroenterol*. 2009; 25:342–51. [PubMed: 19417644]
46. Shaheen NJ, et al. Radiofrequency ablation in Barrett's esophagus with dysplasia. *N Engl J Med*. 2009; 360:2277–88. [PubMed: 19474425]
47. Shaheen NJ, et al. Durability of radiofrequency ablation in Barrett's esophagus with dysplasia. *Gastroenterology*. 2011; 141:460–8. [PubMed: 21679712]
48. Pouw RE, et al. Properties of the neosquamous epithelium after radiofrequency ablation of Barrett's esophagus containing neoplasia. *Am J Gastroenterol*. 2009; 104:1366–73. [PubMed: 19491850]
49. Odze RD, Lauwers GY. Histopathology of Barrett's esophagus after ablation and endoscopic mucosal resection therapy. *Endoscopy*. 2008; 40:1008–15. [PubMed: 19065484]
50. Kauttu T, et al. Long-term results of ablation with antireflux surgery for Barrett's esophagus: a clinical and molecular biologic study. *Surg Endosc*. 2012; 26:1892–7. [PubMed: 22219010]
51. Jovov B, et al. Sub-optimal barrier function in neosquamous epithelium following ablative therapy. *Gastroenterology*. 2011; 140:S218.
52. Zendehdel N, et al. The role and frequency of glutathione s-transferase P1 polymorphism in Iranian patients affected with reflux esophagitis. *Dis Esophagus*. 2010; 23:603–7. [PubMed: 20459448]

Summary Box

1. What is already known about this subject?

- a. Constitutive activation of Nrf2 in Keap1^{-/-} mice leads to esophageal hyperkeratosis.
- b. No esophageal phenotype has been reported in Nrf2^{-/-} mice.

2. What are the new findings?

- a. Nrf2 is expressed in normal human esophageal epithelium and is activated in GERD.
- b. Gastroesophageal reflux activates the Nrf2 pathway in the esophageal epithelium of the wild-type mouse as a defense mechanism.
- c. Nrf2 deficiency reduces TEER and increases intercellular space in the esophageal epithelium of Nrf2^{-/-} mice.
- d. Oxidative damage in the esophageal epithelium is enhanced in Nrf2^{-/-} mice.
- e. Mitochondria and ATP biogenesis are reduced in the esophageal epithelium of Nrf2^{-/-} mice.
- f. A major tight junction protein in the esophagus, Cldn4, is down-regulated in the esophageal epithelium of Nrf2^{-/-} mice. Nrf2 binds to the promoter of Cldn4 gene.

3. How might it impact on clinical practice in the foreseeable future?

Pharmacological activation of Nrf2 may enhance esophageal barrier function in gastroesophageal reflux disease.

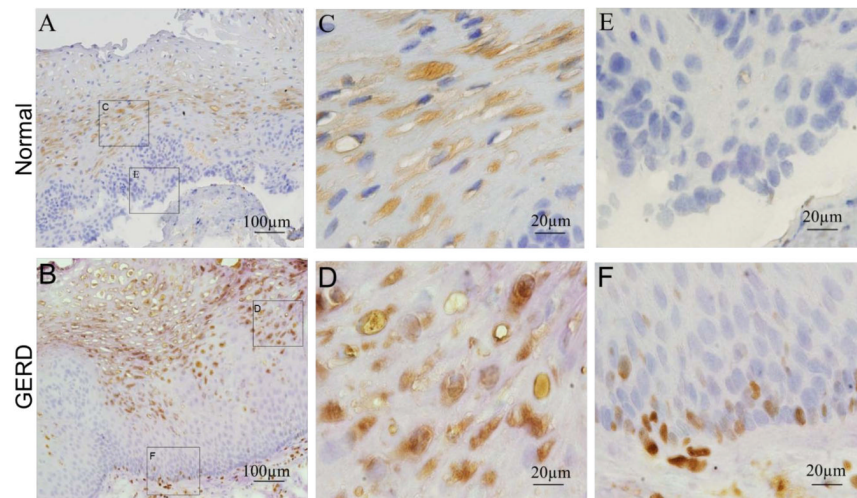


Figure 1.

Expression of Nrf2 in human biopsy tissue of normal esophagus (A, C, E) and GERD (B, D, F). Panel C and E are magnifications of panel A, and panel D and F of panel B. (G)

Expression of HO1 in human biopsy tissue of normal esophagus. (H) Expression of HO1 in human biopsy tissue of GERD. These pictures were representatives of 10 paired samples of normal esophagus and GERD. (I) Percentage of Nrf2 positive cells of total cells. * $P < 0.01$ as compared with normal samples. (J) Percentage of the cells with Nrf2 in nucleus of total positive cells. ** $P < 0.001$ as compared with normal samples.

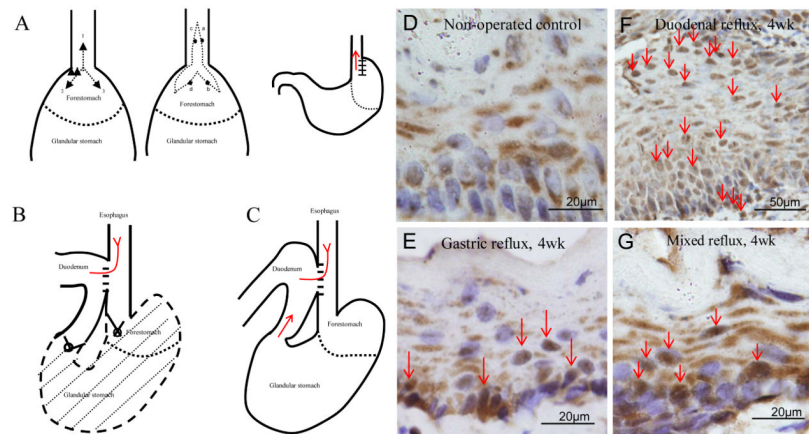


Figure 2.

Activation of Nrf2 in esophageal epithelial cells by gastroesophageal reflux in mice. Gastric reflux (A), duodenal reflux (B) and mixed reflux (C) were induced in mice by esophagogastric anastomosis, esophagogastrroduodenal anastomosis plus gastrectomy, esophagogastrroduodenal anastomosis, respectively. Immunostaining showed over-expression and nuclear localization of Nrf2 in esophageal epithelial cells 4 weeks after gastric reflux (E), duodenal reflux (F) and mixed reflux (G) (red arrows). (D) Non-operated control of Nrf2. (H) Percentage of Nrf2 positive cells of total cells. * $P < 0.05$ as compared with wild-type mice. ** $P < 0.001$ as compared with wild-type mice. (I) Percentage of nuclear stained cells of total positive cells. ** $P < 0.001$ as compared with wild-type mice. Immunostaining for HO1 in esophageal epithelial cells 4 weeks after gastric reflux (K), duodenal reflux (L) and mixed reflux (M). (J) Non-operated control of HO1. These pictures were representatives of 3 samples of each group.

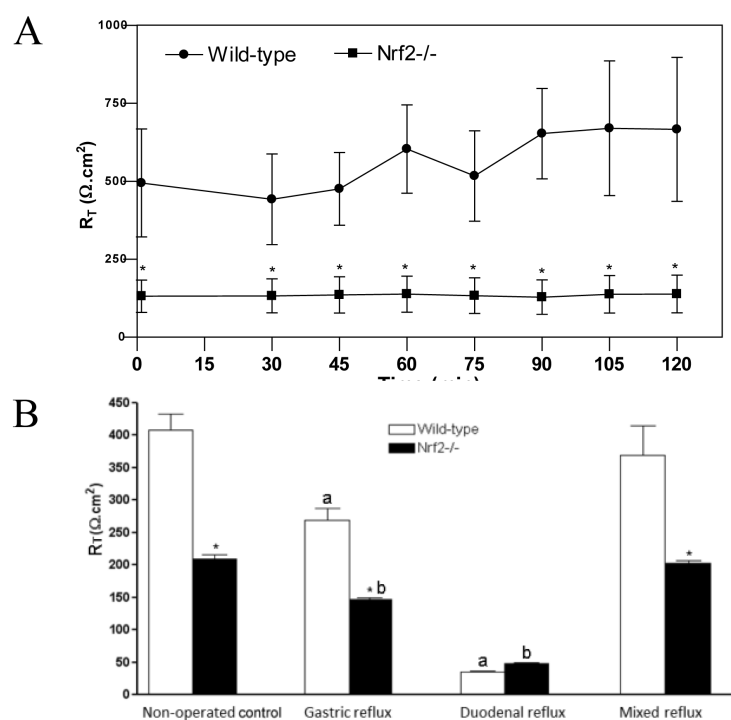


Figure 3.

Impaired barrier function of the esophageal epithelium in Nrf2^{-/-} mice. (A) TEER of mouse esophageal epithelium (means ± SE; n = 6 per group). *P < 0.001 compared to wild-type controls. (B) Effect of gastric, duodenal or mixed reflux for 4 weeks on TEER of the esophageal epithelium in wild-type and Nrf2^{-/-} mice (means ± SE; n = 3 per group). *P < 0.001 compared to wild-type/same surgery; ^aP < 0.01 compared to wild-type/non-operated control; ^bP < 0.01 compared to Nrf2^{-/-}/non-operated control.

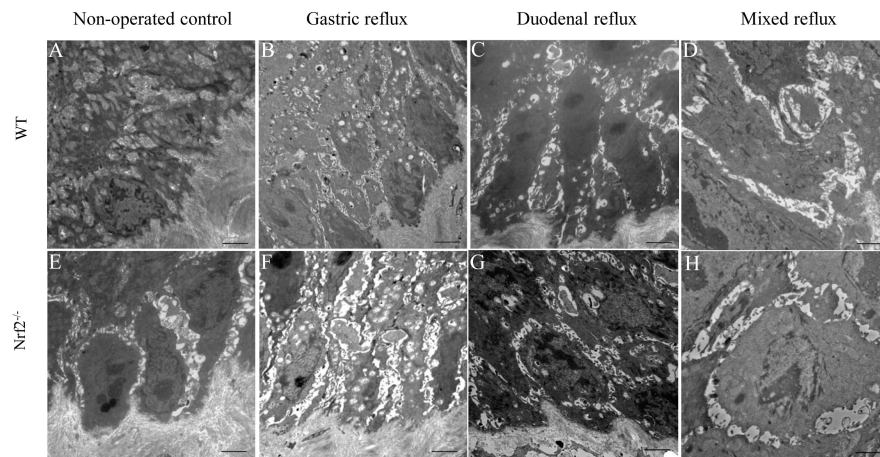


Figure 4.

Morphology and quantification of the ultrastructural changes in the basal cell layer under TEM (magnification 4,400x; size bar = 2 μ m). (A) Wild-type, non-operated control; (B) Wild-type, gastric reflux; (C) Wild-type, duodenal reflux; (D) Wild-type, mixed reflux; (E) *Nrf2*^{-/-}, non-operated control; (F) *Nrf2*^{-/-}, gastric reflux; (G) *Nrf2*^{-/-}, duodenal reflux; (H) *Nrf2*^{-/-}, mixed reflux. (I) Intercellular space (ICS) between basal cells was measured using Olympus MicroSuite Biological Suite and statistic analyzed (n=3 per group). ** $P < 0.01$ compared to wild-type/non-operated control; ^a $P < 0.01$ compared to wild-type/gastric reflux; ^b $P < 0.05$ compared to wild-type/mixed reflux. (B) Density of electron-dense material between basal cells was measured using Olympus MicroSuite Biological Suite and statistic analyzed (n=3 per group). * $P < 0.05$, ** $P < 0.01$, *** $P < 0.001$ compared to wild-type/non-operated control; [¶] $P < 0.001$ compared to wild-type/gastric reflux.

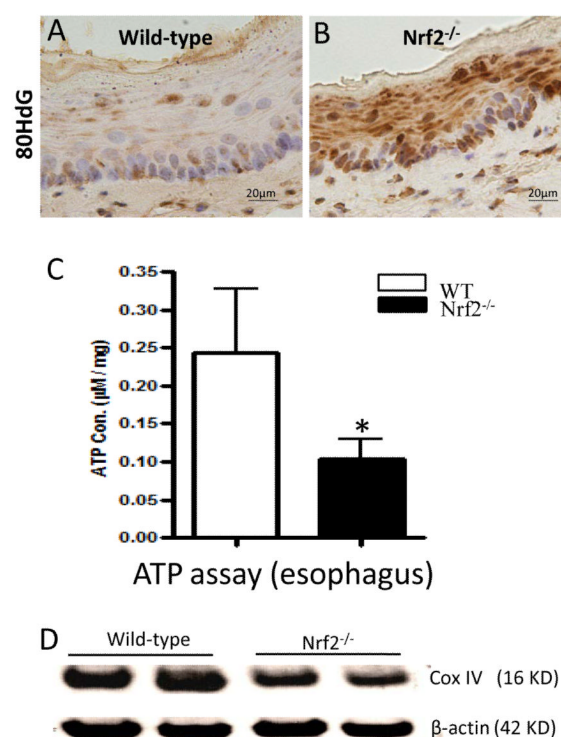


Figure 5.

Increase of oxidative damage and decrease of mitochondrial function in the esophageal epithelium of *Nrf2*^{-/-} mice. (A) Immunostaining of 8OHdG in the esophageal epithelium of wild-type mice; (B) Immunostaining of 8OHdG in the esophageal epithelium of *Nrf2*^{-/-} mice; (A') and (B') are magnified pictures showing nuclear staining (red arrows); (C) ATP concentration in the esophageal epithelium. * $P < 0.01$ compared to wild-type mice. (D) Western blotting for a mitochondrial marker protein, Cox IV. (E) Quantification of the IHC results (A, B). ** $P < 0.001$. (F) Quantification of the Western blotting results (D), ** $P < 0.001$.

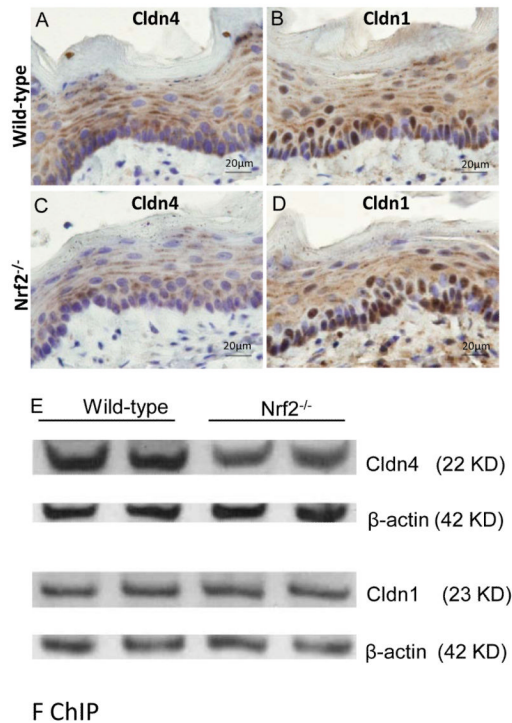


Figure 6.

Expression of Cldn4 and Cldn1 in the esophageal epithelium of *Nrf2*^{-/-} mice. (A, C) Immunostaining for Cldn4; (B, D) Immunostaining for Cldn1. the arrows indicate the cell membrane. (E) Western blotting for Cldn4 and Cldn1; (F) ChIP analysis of Cldn4. Nqo1 serves as a positive control of Nrf2 target gene, and p63 as negative control for potential contamination by genomic DNA. (A'), (B'), (C'), (D') are the magnified pictures showing the staining on cell membrane.